

## **Remote Sensing of Cloud Microphysical Properties with Satellite Data**

---

### Summary and purpose of paper

This paper is to present CGMS results of cloud experiment with satellite data conducted in NSMC of China/CMA.

---

## **Remote Sensing Cloud Microphysical Properties with Satellite Data**

Jian Liu

National Satellite Meteorological Center, Beijing 100081, China

[jianL@nsmc.cma.gov.cn](mailto:jianL@nsmc.cma.gov.cn)

It is well known that clouds are a strong modulator of short wave and long wave components of the earth's radiation budget. It is also recognized that knowledge of cloud properties and their variation in space and time is critical to studies of global climate change. Cloud properties may be expressed by some parameters such as particle size distribution, effective particle radius, thermodynamic phase and water content. Study of cloud optical properties is important for understanding the global climate system.

Here we introduce the work carried out in CMA/NSMC by this paper.

### 1. Cloud Detection

The purpose of cloud detection is to identify pixels containing cloud. It is the first and critical step in our algorithm of operational cloud properties detection. The visible, near-infrared and infrared channel data were used to detect cloud. The detection approach includes threshold detection, statistic analysis, histogram analysis and so on. Clouds are generally characterized by higher reflectance and lower temperature than the underlying earth surface. Because of this, a simple threshold approach with the visible and infrared window channels offer good skill in cloud detection. However, some surface conditions will make this approach inappropriate, most notably over snow and ice. In addition, some cloud types such as thin cirrus, low stratus at night, and small cumulus are difficult to detect because of insufficient contrast with the surface radiance. Cloud edges cause further difficulty since the instrument's field of view is not always completely cloudy or clear. For these reasons, we must as well use other approaches to process. Figure 1 is an example of cloud detection result.

### 2. Cloud microphysical properties analyses

#### 1) Phase analysis

Radiative properties of clouds are determined by their geometric characteristics and their single scattering properties. Single scattering properties of

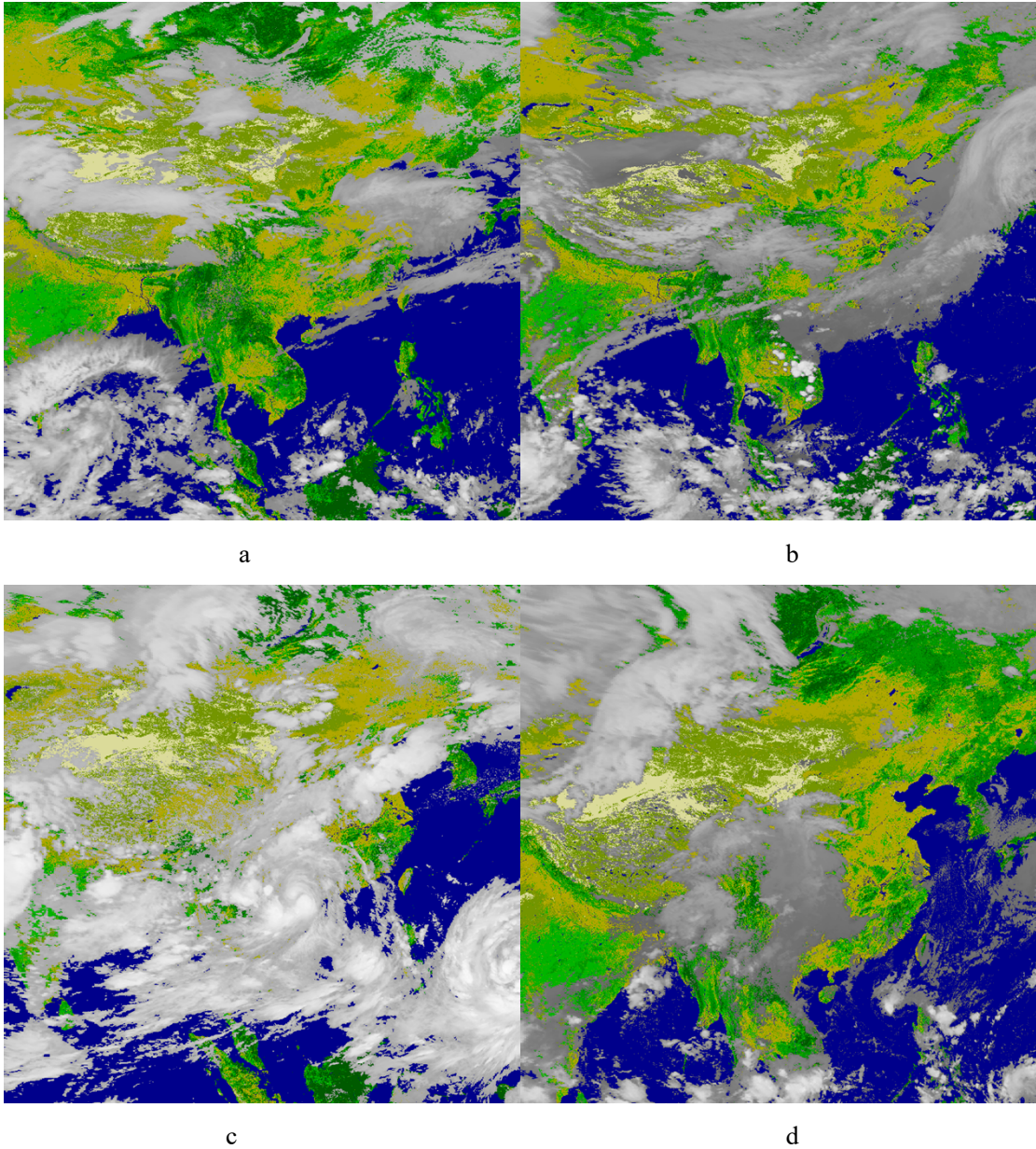


Fig 1. cloud detection results a January b April c July d October

cloud particles are defined by the complex index of reflection ( $m=m_r-im_i$ ), the particle size distribution and the particle shape distribution.

Physical principles guiding the use of 8.52 $\mu\text{m}$ , 11 $\mu\text{m}$ , and 12  $\mu\text{m}$  channels for discriminating liquid water from ice clouds depend upon the bulk and single scattering properties of water droplets and ice crystals. A brief examination of cloud particle absorption and scattering properties follows. The divergence in  $mi$  at wavelengths greater than 9.5  $\mu\text{m}$  forms the basis for the trispectral technique to infer particle thermodynamic phase. The absorption coefficient  $\kappa$  increases more between 8 $\mu\text{m}$  and 11  $\mu\text{m}$  than between 11 $\mu\text{m}$  and 12  $\mu\text{m}$  for ice, but the opposite is true for water. *Strabala et al.* [1994] demonstrated that radiances of ice clouds and water clouds tend to separate when brightness temperature differences (BTD) between 8.5  $\mu\text{m}$  and 11  $\mu\text{m}$  (BTD(8.5-11)) and 11  $\mu\text{m}$  and 12  $\mu\text{m}$  BTD(11-12) are compared. Ice clouds tend to have greater values of BTD(8.5-11) than BTD(11-12) whereas water



the solar zenith angle;  $\mu = |\cos\theta|$ ,  $\theta$  is the zenith angle measured with respect to the positive  $\tau$  direction;  $\phi$  is the relative azimuth angle between the direction of propagation of the emerging radiation and incident solar direction;  $r_e$  is effective particle radius, defined by [8]:

$$r_e = \int_0^{\infty} r^3 n(r) dr / \int_0^{\infty} r^2 n(r) dr \quad (2)$$

where  $n(r)$  is the particle size distribution and  $r$  is the particle radius.

When the optical thickness of the atmosphere is sufficiently large, numerical results for the reflection function must agree with known asymptotic expressions for very thick layers<sup>[9]</sup>. Numerical simulations as well as asymptotic theory show that the reflection properties of optically thick layers depend essentially on two parameters, the scaled optical thickness  $\tau'_c$  and the similarity parameter  $s$ , defined by

$$\tau'_c = (1 - \omega_0 g) \tau_c \quad (3)$$

$$s = \left( \frac{1 - \omega_0}{1 - \omega_0 g} \right)^{1/2} \quad (4)$$

where  $g$  is the asymmetry factor and  $\omega_0$  is the single scattering albedo of a small volume of cloud air. In addition, the reflectance properties of the Earth-atmosphere system depend on the reflectance (albedo) of the underlying surface,  $A_g$ . The similarity parameter, in turn, depends primarily on the effective particle radius.

For a band with a finite bandwidth, Eq. (1) must be integrated over wavelength and weighted by the band's spectral response  $f(\lambda)$  as well as by the incoming solar flux  $F_0(\lambda)$ . Hence, we can rewrite Eq. (1) as

$$R(\tau_c, r_e; \mu, \mu_0, \phi) = \frac{\int R^\lambda(\tau_c, r_e; \mu, \mu_0, \phi) f(\lambda) F_0(\lambda) d\lambda}{\int f(\lambda) F_0(\lambda) d\lambda} \quad (5)$$

From above equations, we knew that values of the reflection function must be stored at three geometrical angles  $(\theta_0, \theta, \phi)$ ,  $M$  optical thickness ( $\tau_c$ ),  $N$  prescribed effective particle radii ( $r_e$ ), and  $K$  surface albedo ( $A_g$ ). This forms a rather large lookup table.

In order to calculate cloud optical thickness and effective particle radius, it is first necessary to compute the reflection of FY-1D channel 1 and channel 6 and brightness temperature of channel 3 for the standard problem of plane-parallel homogeneous cloud layers ( $A_g$ ) with various  $\tau$ ,  $r_e = 2(n+1)/4$  for  $n = 5, \dots, 19$ , assuming a model cloud particle size distribution such as a log-normal size distribution. We generated the radiation libraries for various initial values. Then we use interpolation method to find a pair  $(\tau, r_e)$  from radiation library as a retrieved cloud optical thickness and effective particle radius.

We retrieved  $\tau$  and  $r_e$  separately using pairs of bands, an appropriate optical thickness sensitive band (0.65 $\mu\text{m}$ , FY-1D channel 1), together with an appropriate near-infrared band (e.g., 1.6 $\mu\text{m}$ , and 3.75  $\mu\text{m}$ ), since each near infrared band is sensitive to the effective radius at a different depth within the cloud. For water clouds, the effective radius typically increases from cloud base to cloud top, with the 3.75 $\mu\text{m}$  retrieval being the most sensitive to drops high in the cloud and 1.64  $\mu\text{m}$  much lower in the cloud. The effective radius thus obtained in realistic, vertically inhomogeneous clouds, is some compromise in two theoretical effective radiuses.

Figure 3 and 4 shows the calculation results of optical thickness and effective particle radiuses.

We use airplane data to validate the retrieval results. The validation shows that 64.5% pixels have 1 $\mu\text{m}$  effective radius error and 85% pixels retrieved effective radius error is less than 2 $\mu\text{m}$ .

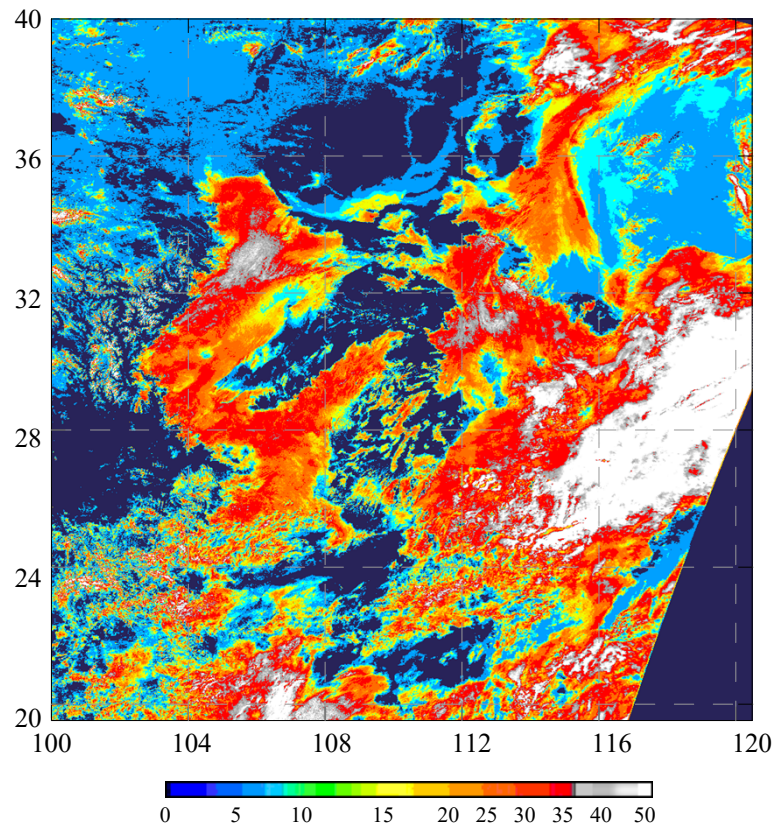


Figure 3 Optical thickness from FY-1D, 22 /11/ 2002

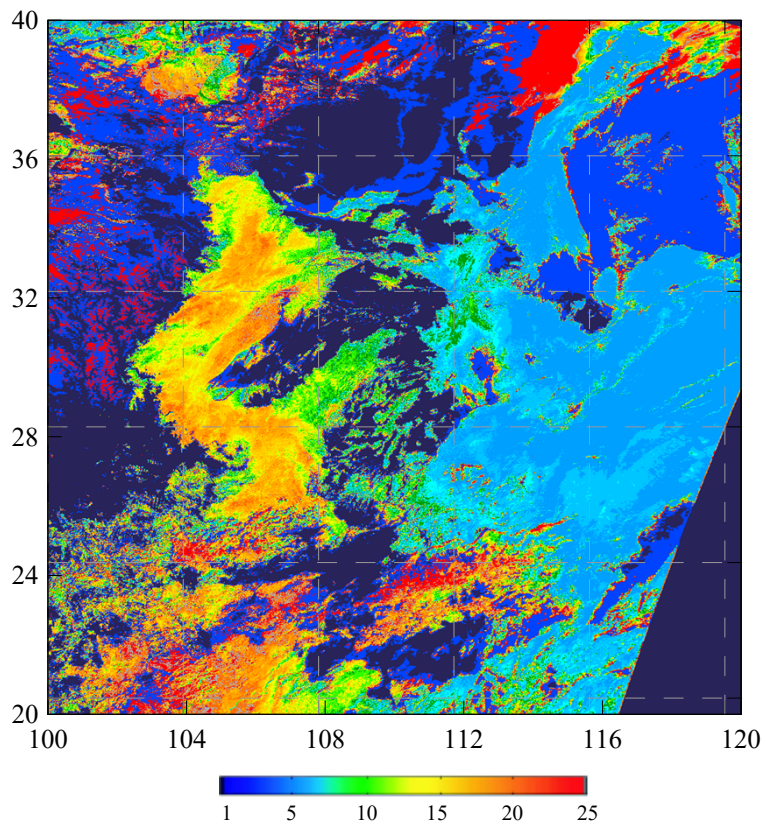


Figure 4 Effective particle radius from FY-1D, 22 /11/2002